

# MedLocker: A Transferable Adversarial Watermarking for Preventing Unauthorized Analysis of Medical Image Dataset

Bangzheng Pu<sup>1,2</sup>, Xingxing Wei<sup>1,2</sup>, Shiji Zhao<sup>2</sup>, and Huazhu Fu<sup>3</sup>

<sup>1</sup> School of Software, Beihang University, Beijing, China. Pu.bangzheng@buaa.edu.cn

<sup>2</sup> Institute of Artificial intelligence, Hangzhou Innovation Institute, Beihang University, Beijing, China. {xxwei, zhaoshiji123}@buaa.edu.cn

<sup>3</sup> Institute of High Performance Computing (IHPC) Agency for Science, Technology and Research (A\*STAR), Singapore. hzfu@ieee.org

**Abstract.** The collection of medical image datasets is a demanding and laborious process that requires significant resources. Furthermore, these medical datasets may contain personally identifiable information, necessitating measures to ensure that unauthorized access is prevented. Failure to do so could violate the intellectual property rights of the dataset owner and potentially compromise the privacy of patients. As a result, safeguarding medical datasets and preventing unauthorized usage by AI diagnostic models is a pressing challenge. To address this challenge, we propose a novel visible adversarial watermarking method for medical image copyright protection, called MedLocker. Our approach involves continuously optimizing the position and transparency of a watermark logo, which reduces the performance of the target model, leading to incorrect predictions. Importantly, we ensure that our method minimizes the impact on clinical visualization by constraining watermark positions using semantical masks (WSM), which are bounding boxes of lesion regions based on semantic segmentation. To ensure the transferability of the watermark across different models, we verify the cross-model transferability of the watermark generated on a single model. Additionally, we generate a unique watermark parameter list each time, which can be used as a certification to verify the authorization. We evaluate the performance of MedLocker on various mainstream backbones and validate the feasibility of adversarial watermarking for copyright protection on two widely-used diabetic retinopathy detection datasets. Our results demonstrate that MedLocker can effectively protect the copyright of medical datasets and prevent unauthorized users from analyzing medical images with AI diagnostic models.

**Keywords:** Visible watermarking · Copyright protection · Adversarial attack · Transferability.

## 1 Introduction

Production of medical image datasets necessitates the participation of experienced radiologists and costly imaging equipment. Furthermore, it may undergo

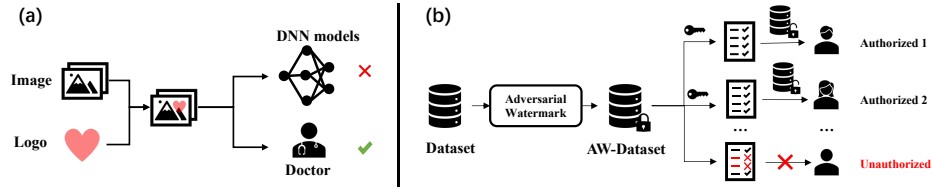


**Fig. 1.** (a) Our goal is to generate watermarks on medical images to prevent unauthorized analysis of datasets, while minimizing interference with clinical diagnosis. (b) Besides, our method should distinguish and verify the authorized users.

a substantial duration to amass sufficient cases or procure data simultaneously from multiple healthcare institutions [19]. Unauthorized AI diagnostic models to analyze medical imaging data may lead to the disclosure of patient privacy, infringement of intellectual property and copyright, inaccurate diagnoses, and ethical issues. In the past, the common method for protecting the ownership of images is adding watermarks, such as visible watermarking [20,11,8,13] or invisible digital watermarking [15,1,23,22]. However, these traditional methods are only effective for human declarations of copyright but are unable to prevent images from being analyzed by AI models.

Recently, adversarial examples put a threat to deep neural networks as they can cause models to make incorrect predictions [4,28]. Adversarial watermarks leverage this characteristic to prevent data infringement by DNN models. Tian et al. [25] create imperceptible adversarial watermarks to confound label-image mapping, to prevent private images collection from unapproved DNN on the internet. Backdoor watermarking [5,26] is used to protect the copyright of the authorized model by correlating specific categories with a trigger. These adversarial watermarks that associated with specific categories are easier to be detected. Li et al. [12] propose an untargeted backdoor watermark to improve the stealthiness and verify ownership by hypothesis testing. Different from meaningless watermarks from the above research, Jia et al. [10] propose a query-based method to generate meaningful adversarial watermarks. For medical images, Ma et al. [14] evaluate the adversarial noise against several disease classifiers and Ozbulak et al. [17] propose an adaptive mask attack against the segmentation network. However, diffusion models [16] have been prove to be powerful for purifying adversarial noise, but implement less effect on meaningful information of images. Moreover, these watermarks are difficult to prevent the utilization of diagnostic models with unknown information.

To address above issues, we propose a **visible adversarial watermark method called MedLocker for protecting copyrights of medical images**, as shown in Fig. [1]. Our method not only misleads the predictions of unauthorized diagnostic models but also displays meaningful logos to claim ownership in the medical image. Adversarial watermarks are generated by querying source models' outputs, and the locations and transparency of the watermark logo are optimized by the evolutionary algorithm. Since the information of medical diag-

nostic models in practice is unknown, transferred attacks are implemented, and transferability is improved by the ensemble model. Furthermore, reliable medical disease diagnosis relies on prior knowledge of anatomy, and to address this, we propose **a method of semantic masked lesion adversarial watermarking for medical datasets (WSM)**. We obtain the location of lesions in advance using an image segmentation model, and our semantic masks can limit the watermark away from areas with diagnostic meaning, which does not affect the analysis by doctors. we evaluate the performance of our proposed method using various mainstream backbones on two widely-used diabetic retinopathy detection datasets. Our results demonstrate that MedLocker can effectively prevent unauthorized users from analyzing medical images with AI models. Additionally, we discuss the watermarking certification method, which ensures the ability to distinguish and unlock authorized datasets. **Our code implementation will be publicly available after acceptance.**

## 2 Proposed Method

Our goal is to add watermarks to images and prevent the unauthorized analysis of medical datasets while minimizing interference with doctors’ judgments (Fig. [1]). Our MedLocker has two main settings: watermarks in arbitrary positions (WAP) and watermarks limited by semantic masks (WSM).

### 2.1 MedLocker Creation in General Settings

**The Visible Watermark:** We use the alpha blending technique [20] to composite watermarks. Given an original image of size  $W \times H$  with four channels *RGBA* and a watermark logo of size  $M \times N$  with the same channels, the alpha blended pixel is formulated as follows,

$$I(i, j) = (1 - \alpha/255) \times I_{ori}(i, j) + \alpha/255 \times I_{logo}(p, q), \quad (1)$$

where  $I_{ori}$  represents the original image,  $I_{logo}$  is the watermark logo image,  $I$  is the blended image,  $\alpha$  represents the pixel value of the alpha channel,  $\alpha \in [0, 255]$ . Assuming the coordinate of the upper-left is the origin point,  $i \in [0, W], j \in [0, H]$ . let  $x$  and  $y$  be the coordinates of the upper-left of the watermark logo on the original image,  $p \in [x, x + M], q \in [y, y + N], x \in [0, W - x), y \in [0, W - y)$ . The size of the watermark logo is recalculated based on the original image size and the scaling factor  $sl$ , which can be expressed as,

$$[M', N'] = \min(W/(sl \times M), H/(sl \times N)) \times [M, N]. \quad (2)$$

**Optimization Objective:** As illustrated in Fig. [2], our approach involves generating adversarial watermarks for each sample in the dataset by querying the source model, followed by optimizing the location  $(x, y)$  and transparency  $\alpha$

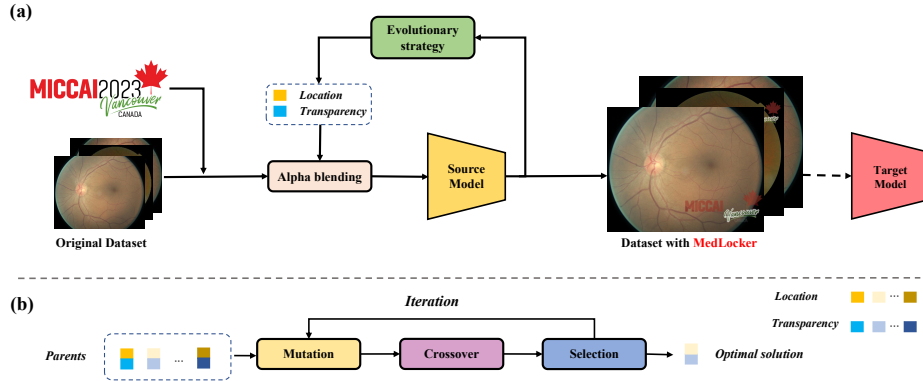


**Fig. 2.** The flowchart of our MedLocker. (a) The dataset with MedLocker is generated by optimizing adversarial watermarks on source models, whose transferability is evaluated on target models; (b) The evolutionary strategy is used to optimize the parameters of alpha blending.

using an evolutionary algorithm. Specifically, we generate dominant individuals  $[\alpha, x, y]$  that minimize the ground-truth class probability  $f_t(I_n)$  for the  $n$ -th sample. Mathematically, this can be expressed as follows,

$$\text{minimize } f_t(I_n(\alpha, x, y)), \quad \text{s.t. } \alpha \in [0, 255], x \in [0, W - x), y \in [0, W - y). \quad (3)$$

**Evolutionary Algorithm:** Due to the fact that transparency is a continuous variable and position is a discrete variable, we address this issue by using Evolution Strategy, which has strong global search capability and adaptability. Initially, we randomly initialize a set of individuals as parents ( $X_{i,g} = [\alpha, x, y]$  represents the  $g$ -th generation of the  $i$ -th individual, where  $i \in \{1, 2, \dots, N_p\}$  and  $g \in \{1, 2, \dots, N_g\}$ ), and evaluate the fitness of each individual based on the classification confidence  $f(I_n)$ . We then use Basing Hopping (BH) [10] with a few iterations to generate beneficial mutations in the offspring.

$$M_{i,g} = BH(X_{i,g}, N_{iter}, s) \quad (4)$$

where  $N_{iter}$  is the iteration number and  $s$  is the mutation step.

Then a crossover operation is performed between the parents and the mutated offspring with a certain crossover rate  $CR$  to enrich the genetic diversity and generate new combinations,

$$C_{i,g,j} = \begin{cases} M_{i,g,j}, & \text{if } \text{rand}(0, 1) \leq CR, \\ X_{i,g,j}, & \text{Otherwise.} \end{cases} \quad (5)$$

where  $X_{i,g,j}$  represents  $j$ -th gene of  $X_{i,g}$ .

Finally, the dominant individuals are selected by comparing  $f_t(I_n)$ ,

$$S_{i,g} = \begin{cases} C_{i,g}, & \text{if } f_t[I_n(C_{i,g})] \leq f_t[I_n(X_{i,g})], \\ X_{i,g}, & \text{Otherwise.} \end{cases} \quad (6)$$

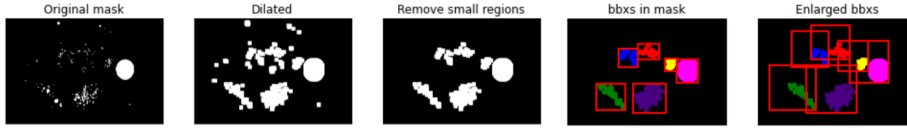


**Fig. 3.** The process of generating semantic masks begins by creating a pixel-level mask that delineates the lesion regions within the image. Next, we use this mask to derive a set of bounding boxes (bbxs) that serve to constrain the position of the regions of interest.

Thus, by blending the watermark logo with the original image according to the optimal individuals, we can eventually create the MedLocker of our dataset.

## 2.2 MedLocker Limited by Semantic Mask (WSM)

Lesion grading based on pathological features is crucial for accurate diagnosis. To minimize the visual impact of watermarks, we propose a mask-generation method that utilizes semantic information from medical images to avoid occlusion. As depicted in Fig. [3], our approach comprises the following steps:

**STEP 1:** Obtaining a pixel-level mask  $M_n \in 0, 1$  of the fundus lesion via a segmentation network.

**STEP 2:** Utilizing dilated convolution  $K(size, n_{iter}) \otimes M_n$  to group adjacent smaller pixels into connected regions  $R = \{r_1, r_2, \dots, r_m\}$ , where  $size$  is the kernel size and  $n_{iter}$  is the iteration number.

**STEP 3:** Removing small isolated regions with an area below a threshold  $\lambda$ , denoted as  $r_i = 0$  if  $A_{r_i} \leq \lambda$ , where  $A_{r_i}$  represents the area of  $r_i$ .

**STEP 4:** Calculating the bounding boxes  $B$  of the remaining regions, represented as a tetrad  $(x, y, w, h)$ . In the case of bounding boxes with high overlap ( $IOU(B_k, B_l) > \gamma$ ), they are merged. The merged box in the  $j$ -th comparison can be expressed as follows,

$$B_{merged,j} = ((\min(x_k, x_l), \min(y_k, y_l), \max(w_k, w_l), \max(w_k, w_l))). \quad (7)$$

**STEP 5:** As the watermark logo's top-left vertex position is represented by  $(x, y)$ , expanding the bounding boxes upwards and leftwards by the width and length of the watermark logo is necessary.

## 2.3 Transferable Adversarial Watermark

The information of medical diagnosis models in practical scenarios is often unknown. Therefore, it is crucial to assess the transferability of our watermarking method on various backbone models, in the hope that the adversarial watermark generated on the source model can also be effective on the target model. To enhance transferability, we employ an ensemble model during watermark generation and launch attacks on it. The confidence score of the  $n$ -th image in the

ensemble model can be formulated as,

$$f(I_n)_{ensemble} = \sum_{i=1}^k \beta_i f_i(I_n), \quad (8)$$

where  $k$  is the number of models, and  $\beta$  is the weight of single model.

**Authorization for Datasets:** During the deployment, the datasets can be accessed through a unique key, which is a specialized document of watermarking parameters assigned to each authorized user,  $Key = \{I_1 : [L_1, x_1, y_1], I_2 : [L_2, x_2, y_2], \dots, I_n : [L_n, x_n, y_n]\}$ ,  $L = \{\alpha_1, \alpha_2, \dots, \alpha_m\}$ ,  $m \in [1, M \times N]$ . In order to remove the watermarks, authorized users may employ an inverse alpha blending operation, as:

$$I_{ori}(i, j) = (I(i, j) - \alpha/255 \times I_{logo}(p, q))/(1 - \alpha/255). \quad (9)$$

### 3 Experiments

**Datasets:** We select two diabetic retinopathy (DR) datasets (EyePAC on Kaggle [3] and IDRiD [18]) to validate our method. The images in both datasets contain labels for DR grading (no DR, mild, moderate, severe, and proliferative DR). In addition, IDRiD contains fundus lesion data used to train the semantic segmentation model.

**Models training:** The source model represents the model used for generating adversarial watermarks. The target model represents the model under transferred attack. We use the EyePAC dataset to train mainstream backbones as our source model for watermarking attacks. Specifically, we split the training and testing sets as a 3:1 ratio. Due to the unbalanced categories, 500 images of each category is evenly sampled as the training set for training the DR classification models of ResNet18 [6], VGG16 [21], Inceptionv3 [24], MobileNetv3 [7], ResNet50 [6], Densenet121 [9], and ViT [2]. IDRiD segmentation dataset lacks the labels of DR grading but includes pixel-level labels of lesions, so this part of the data is graded as DR, and all classified data is relabeled as two classes (No DR or DR). We train the binary classifier with resnet18 and follow the [27] settings to train the semantic segmentation model with an UNet++ [29].

**Watermark generation:** We randomly sample 150 images from each category on the pre-processed EyePAC dataset, which is cropped and resized. To verify cross-model transferability, we only attack samples that are successfully classified by all networks. In experiments of MedLocker with semantic mask limit, we relabel 80 images from the IDRiD segmentation dataset as DR and sample 80 No DR images from the classification dataset. Our watermark generation experiments follow a unified hyperparameter setting:  $sl = 4, N_p = 50, N_g = 3, CR = 0.9, s = 10, \alpha \in [100, 255], N_{iter} = 3$ . The generation of our semantic masks followed:  $K(10, 10), a = 5 \times 10^4, \gamma = 0.5$ .

**Metrics:** Accuracy is used to measure classifiers' performance and attack success rate (ASR) is used to evaluate adversarial watermarks. ASR is equal to

**Table 1.** Watermarks in EyePAC against source models

Source model	ResNet18	VGG16	Inceptionv3	MobileNetv3	ResNet50	DenseNet121	ViT	Ensemble
ASR	71.69%	72.88%	50.00%	60.89%	55.92%	66.96%	67.26%	52.05%

**Table 2.** Watermarks in EyePAC against target models

Source model	Target model							
	ResNet18	VGG16	Inceptionv3	MobileNetv3	ResNet50	DenseNet121	ViT	Ensemble
ResNet18	-	91.10%	64.83%	69.91%	69.49%	67.01%	83.25%	70.34%
VGG16	80.83%	-	54.89%	65.41%	63.16%	60.96%	74.56%	64.29%
Inceptionv3	73.91%	81.64%	-	70.53%	69.08%	71.62%	79.72%	74.88%
MobileNetv3	72.69%	76.65%	55.07%	-	74.01%	77.66%	73.4%	69.6%
ResNet50	72.25%	74.01%	58.15%	74.01%	-	83.42%	78.39%	68.72%
DenseNet121	62.6%	65.85%	55.04%	69.51%	73.58%	-	69.1%	52.44%
ViT	74.89%	79.15%	57.87%	70.21%	74.04%	72.34%	-	65.53%
Ensemble	-	-	-	-	82.11%	78.71%	80.91%	-

**Table 3.** ASR of Watermarks in IDRiD

	WAP		WSM-in bbxs	WSM-out bbxs
	DR	No DR	DR	DR
Basing Hoping	72.06%	73.53%	11.69%	18.18%
Radom Mutation	2.59%	58.82%	12.98%	2.59%

the number of samples successfully attacked, divided by the number of samples correctly predicted.

**Result of MedLocker in general settings:** Table 1 shows the ASR of adversarial watermarks by querying source models, the ensemble model including resnet18, vgg16, inceptionv3, and mobilenetv3, whose weighting parameters  $\beta_i = 0.25$ . Table 2 shows the ASR of transferable adversarial watermarks, which come from the samples that successfully attacked source models. We show the results of transferable attacks more intuitively with the average data in Fig. [4](b). The average ASR of the source model represents the performance of adversarial watermarks generated by the source model, the ensemble model achieve 80.58%, and the second is inceptionv3 74.48%. The average accuracy of the target model shows the robustness of target models against watermarks, among which inceptionv3 has the best accuracy 42.36%, followed by the ensemble model 33.46%. The results show that it is beneficial to improve the transferability of watermarks by ensemble models.

**Result of MedLocker limited by semantic masks:** In this part, our experiments perform on the IDRiD dataset and ResNet18. As shown in Fig. [3], we calculate the boundaries of the lesion region from the mask output of the segmentation network. Our watermark positions obey three settings, WAP: watermarks in arbitrary positions; WSM-in bbxs: watermarks in bounding boxes; WSM-out bbxs: watermarks out of bounding boxes. Since the bounding box only constrains images with the ground truth of DR, we show the ASR of DR and No DR separately, as shown as Table 3. The results show that the watermark outside the bounding boxes can also reach 18.18% ASR. WAP is more threatening to models while WSM-in bbxs provide less visual occlusion of lesion regions.

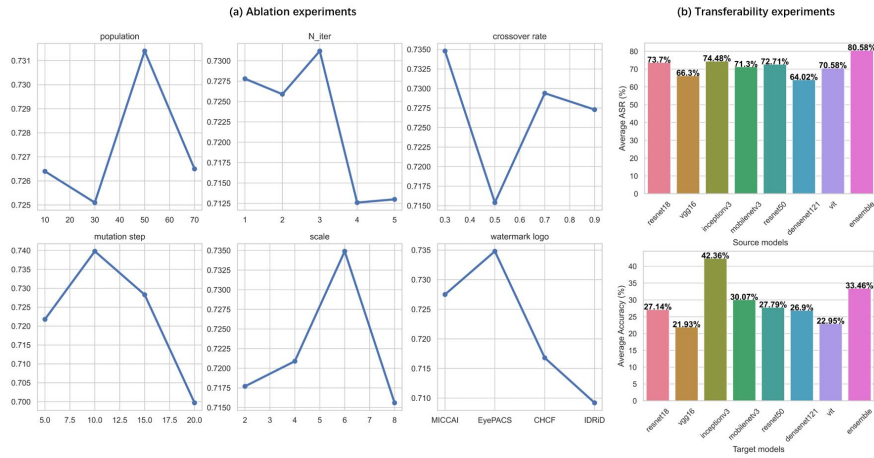


**Fig. 4.** (a) Ablation study is performed in resnet18. The horizontal axis is the change in the corresponding parameter, the vertical axis is average ASR of the two datasets, the rest parameters follows the general settings of section 3.1.; (b) Average performance of transferable adversarial watermarks. **Source model**: the average transferred ASR of watermarks generated by source models; **Target model**: the average accuracy of target models under transferred attack.

To verify the effectiveness of our strategy which uses basin hopping for directional mutation, we compare the ASR with a random mutation following the same hyperparameter for comparison. The results show that the basing hopping algorithm improves the ASR under the same attack settings, especially without the bbxs constraint.

**Ablation study:** We also perform the ablation study to analyze appropriate hyperparameter settings: where the optimization related includes population number, BH iteration, crossover rate, and mutation step; where the watermark related includes scaling ratio of the watermark and the type of logo. Fig. [4](a) shows the results, where our parameter setting performs a good ASR in a dynamic range.

## 4 Conclusion

In this paper, we propose MedLocker, a novel visible adversarial watermarking method for protecting medical image copyrights. Our approach involves the use of meaningful watermarking logos to prevent unauthorized analysis by diagnostic models, while minimizing visual interference to doctors. We conduct experiments to demonstrate the broad applicability of our approach, transferring attacks across different backbones and using an ensemble model as the source model to improve transferability. Furthermore, our semantic mask can restrict the active region of the watermark and significantly reduce model prediction accuracy, even outside the lesion area. By introducing a visible watermark, we



enable copyright protection while ensuring that medical practitioners can still access and interpret images accurately. Our findings emphasize the potential of adversarial watermarking as an effective measure for safeguarding sensitive medical data, and we hope that our work will inspire further research in this area.

## References

1. Allaf, A.H., Kbir, M.A.: A review of digital watermarking applications for medical image exchange security. In: *Innovations in Smart Cities Applications Edition 2: The Proceedings of the Third International Conference on Smart City Applications*. pp. 472–480. Springer (2019)
2. Dosovitskiy, A., Beyer, L., Kolesnikov, A., Weissenborn, D., Zhai, X., Unterthiner, T., Dehghani, M., Minderer, M., Heigold, G., Gelly, S., Houlsby, N.: An image is worth 16x16 words: Transformers for image recognition at scale. In: *Proceedings of the IEEE/CVF conference on computer vision and pattern recognition*. pp. 3156–3164 (2021)
3. Emma Dugas, Jared, J., Cukierski, W.: Diabetic retinopathy detection (2015), <https://kaggle.com/competitions/diabetic-retinopathy-detection>
4. Finlayson, S.G., Bowers, J.D., Ito, J., Zittrain, J.L., Beam, A.L., Kohane, I.S.: Adversarial attacks on medical machine learning. *Science* **363**(6433), 1287–1289 (2019)
5. Gu, T., Liu, K., Dolan-Gavitt, B., Garg, S.: Badnets: Evaluating backdooring attacks on deep neural networks. *IEEE Access* **7**, 47230–47244 (2019)
6. He, K., Zhang, X., Ren, S., Sun, J.: Deep residual learning for image recognition. In: *Proceedings of the IEEE conference on computer vision and pattern recognition*. pp. 770–778 (2016)
7. Howard, A.G., Zhu, M., Chen, B., Kalenichenko, D., Wang, W., Weyand, T., Andreetto, M., Adam, H.: Mobilenets: Efficient convolutional neural networks for mobile vision applications. *arXiv preprint arXiv:1704.04861* (2017)
8. Hu, Y., Kwong, S., Huang, J.: An algorithm for removable visible watermarking. *IEEE Transactions on Circuits and Systems for Video Technology* **16**(1), 129–133 (2005)
9. Huang, G., Liu, Z., Van Der Maaten, L., Weinberger, K.Q.: Densely connected convolutional networks. In: *Proceedings of the IEEE conference on computer vision and pattern recognition*. pp. 4700–4708 (2018)
10. Jia, X., Wei, X., Cao, X., Han, X.: Adv-watermark: A novel watermark perturbation for adversarial examples. In: *Proceedings of the 28th ACM International Conference on Multimedia*. pp. 1579–1587 (2020)
11. Kankanhalli, M.S., Ramakrishnan, K., et al.: Adaptive visible watermarking of images. In: *Proceedings IEEE International Conference on Multimedia Computing and Systems*. vol. 1, pp. 568–573. IEEE (1999)
12. Li, Y., Bai, Y., Jiang, Y., Yang, Y., Xia, S.T., Li, B.: Untargeted backdoor watermark: Towards harmless and stealthy dataset copyright protection. *arXiv preprint arXiv:2210.00875* (2022)
13. Liu, T.Y., Tsai, W.H.: Generic lossless visible watermarking—a new approach. *IEEE transactions on image processing* **19**(5), 1224–1235 (2010)
14. Ma, X., Niu, Y., Gu, L., Wang, Y., Zhao, Y., Bailey, J., Lu, F.: Understanding adversarial attacks on deep learning based medical image analysis systems. *Pattern Recognition* **110**, 107332 (2021)

15. Mohanarathinam, A., Kamalraj, S., Prasanna Venkatesan, G., Ravi, R.V., Manikandababu, C.: Digital watermarking techniques for image security: a review. *Journal of Ambient Intelligence and Humanized Computing* **11**, 3221–3229 (2020)
16. Nie, W., Guo, B., Huang, Y., Xiao, C., Vahdat, A., Anandkumar, A.: Diffusion models for adversarial purification. arXiv preprint arXiv:2205.07460 (2022)
17. Ozbulak, U., Van Messem, A., De Neve, W.: Impact of adversarial examples on deep learning models for biomedical image segmentation. In: *Medical Image Computing and Computer Assisted Intervention–MICCAI 2019: 22nd International Conference, Shenzhen, China, October 13–17, 2019, Proceedings, Part II* 22. pp. 300–308. Springer (2019)
18. Porwal, P., Pachade, S., Kamble, R., Kokare, M., Deshmukh, G., Sahasrabudde, V., Meriaudeau, F.: Indian diabetic retinopathy image dataset (idrid) (2018)
19. Rädtsch, T., Reinke, A., Weru, V., Tizabi, M.D., Schreck, N., Kavur, A.E., Pekdemir, B., Roß, T., Kopp-Schneider, A., Maier-Hein, L.: Labelling instructions matter in biomedical image analysis. *Nature Machine Intelligence* (mar 2023)
20. Shen, B., Sethi, I.K., Bhaskaran, V.: Dct domain alpha blending. In: *Proceedings 1998 International Conference on Image Processing. ICIP98 (Cat. No. 98CB36269)*. vol. 1, pp. 857–861. IEEE (1998)
21. Simonyan, K., Zisserman, A.: Very deep convolutional networks for large-scale image recognition. arXiv preprint arXiv:1409.1556 (2014)
22. Soualmi, A., Alti, A., Laouamer, L.: An imperceptible watermarking scheme for medical image tamper detection. *International Journal of Information Security and Privacy (IJISP)* **16** (2022)
23. Soualmi, A., Alti, A., Laouamer, L.: A new blind medical image watermarking based on weber descriptors and arnold chaotic map. *Arabian Journal for Science and Engineering* **43**, 7893–7905 (2018)
24. Szegedy, C., Liu, W., Jia, Y., Sermanet, P., Reed, S., Anguelov, D., Erhan, D., Vanhoucke, V., Rabinovich, A.: Going deeper with convolutions. In: *Proceedings of the IEEE conference on computer vision and pattern recognition*. pp. 1–9 (2015)
25. Tian, Q., Kuang, K., Jiang, K., Liu, F., Wang, Z., Wu, F.: Confoundergan: Protecting image data privacy with causal confounder. arXiv preprint arXiv:2212.01767 (2022)
26. Turner, A., Tsipras, D., Madry, A.: Label-consistent backdoor attacks. arXiv preprint arXiv:1912.02771 (2019)
27. Wang, H., Zhou, Y., Zhang, J., Lei, J., Sun, D., Xu, F., Xu, X.: Anomaly segmentation in retinal images with poisson-blending data augmentation. *Medical Image Analysis* **81**, 102534 (2022)
28. Zhou, Q., Zuley, M., Guo, Y., Yang, L., Nair, B., Vargo, A., Ghannam, S., Arefan, D., Wu, S.: A machine and human reader study on AI diagnosis model safety under attacks of adversarial images. *Nature Communications* **12**(1), 7281 (dec 2021)
29. Zhou, Z., Rahman Siddiquee, M.M., Tajbakhsh, N., Liang, J.: Unet++: A nested u-net architecture for medical image segmentation. In: *Deep Learning in Medical Image Analysis and Multimodal Learning for Clinical Decision Support: 4th International Workshop, DLMIA 2018, and 8th International Workshop, ML-CDS 2018, Held in Conjunction with MICCAI 2018, Granada, Spain, September 20, 2018, Proceedings* 4. pp. 3–11. Springer (2018)